Fractional Extreme Value Adaptive Training Method: Fractional Steepest Descent Approach

Yi-Fei Pu, Ji-Liu Zhou, *Senior Member, IEEE*, Yi Zhang, *Senior Member, IEEE*, Ni Zhang, Guo Huang, Patrick Siarry, *Senior Member, IEEE*

***Abstract*— The application of fractional calculus to signal processing and adaptive learning is an emerging area of research. A novel fractional adaptive learning approach that utilizes fractional calculus is presented in this paper. In particular, a fractional steepest descent approach is proposed. A fractional quadratic energy norm is studied, and the stability and convergence of our proposed method are analyzed in detail. The fractional steepest descent approach is implemented numerically and its stability is analyzed experimentally.**

***Index Terms*— Fractional calculus, fractional differential, fractional energy norm, fractional extreme point, fractional gradient.**

I. Introduction

THE integer-order adaptive learning approaches based on the integer-order calculus, such as the classical first-order steepest descent (FOSD) method, produce time-varying parameters relevant for nonlinear systems by generalizing finite quantity of pattern training. The integer-order adaptive learning approaches automatically adapt to the optimal requirements of non-stationary variations in a system. Furthermore, they can produce improvements in system performance even if the characteristics of input signals are unknown or varying with time [1]–[5]. The FOSD method is a widely used gradient-based approach for optimizing the traditional integer-order pattern recognition, adaptive control, and adaptive signal processing problems. Unlike the traditional integer-order Newton optimization approach, the reverse incremental search employed in the FOSD method is in the opposite direction of the first-order gradient of a quadratic energy norm [1]–[3]. For digital analysis, the quadratic energy norm is a typical choice. However, in most of the actual integer-order adaptive systems, the quadratic energy norm of system is unknown; thus, it should be measured and estimated in accordance with the actual random input data of the integer-order adaptive system. The FOSD method utilizes a filtering process that reduces the noise of gradient measurement errors [4], [5]. The least mean squares (LMS) algorithm based on the FOSD method is simple and effective [6], [7]. Because the LMS algorithm was initially proposed for non-recursive linear filters, its applications were limited. Later, many improved variants of LMS algorithm have also been proposed, like the LMS-Newton algorithm [8], sequential regression algorithm [9], [10], and random searching algorithm [9], [11]. However, the integer-order adaptive learning approaches cannot be used for fractional pattern recognition, adaptive control, or adaptive signal processing. In this paper, a novel fractional adaptive learning (FAL) approach is proposed, which is called the fractional steepest descent approach.

Over the past three hundred years, fractional calculus has become an important branch of mathematical analysis [12]–[15]. Fractional calculus is as old as integral calculus, although, until recently, its utility has been confined to the domain of mathematics only. Fractional calculus is a novel mathematical method that may be useful for physical scientists too. Most of the special functions in mathematical physics involve differintegrable series. Fractional calculus extends and unifies the concepts of difference quotients and Riemann sums [16], [17]. The random variable in a physical process can be deemed as the displacement corresponding to the random movement of particles. Fractional calculus can be used to analyze and process several specific physical problems; in particular, it is useful in fields such as biomedical engineering, diffusion processes, viscoelasticity theory, fractal dynamics, and fractional control [18]–[26]. One main advantage of fractional calculus is that most functions are equivalent to a power series, whereas others are equivalent to the superposition or product of a certain function and a power function [12]–[17]. Unfortunately, the majority of its usage still lies in describing the transient state of physical change. It is seldom used for the processes involving systemic evolution [18]–[30].

The issue of how to efficiently apply fractional calculus for the purpose of signal analysis and signal processing, especially for the purpose of adaptive learning, is an emerging area of research. Till now, several researchers have concentrated in

Manuscript received March 12, 2013; revised October 8, 2013; accepted October 10, 2013. Date of publication December 5, 2013; date of current version March 16, 2015. This work was supported in part by the Foundation Franco-Chinoise Pour La Science Et Ses Applications, in part by the National Natural Science Foundation of China under Grant 60972131 and Grant 61201438, in part by the Returned Overseas Chinese Scholars Project of Education Ministry of China under Grant 20111139, in part by the Science and Technology Support Project of Sichuan Province of China under Grant 2011GZ0201 and Grant 2013SZ0071, in part by the Soft Science Project of Sichuan Province of China under Grant 2013ZR0010, in part by the Scientific and Technical Innovation Seedling Project of Sichuan Province of China under Grant 2012ZZ023, and in part by the Science and Technology Achievements Transformation Project of Chengdu of China under Grant 12DXYB255JH-002.

Y.-F. Pu, J.-L. Zhou, and Y. Zhang are with the School of Computer Science and Technology, Sichuan University, Chengdu 610065, China (e-mail: puyifei@scu.edu.cn; zhoujl@scu.edu.cn; zhangyi@scu.edu.cn).

N. Zhang is with Library, Sichuan University, Chengdu 610065, China (e-mail: zhangni77@yeah.net).

G. Huang is with the College of Computer Science and Technology, Leshan Normal University, Leshan 614000, China (e-mail: huangguoxuli@yeah.net).

P. Siarry is with the Université de Paris 12, Creteil Cedex 94010, France (e-mail: siarry@univ-paris12.fr).

Color versions of one or more of the figures in this paper are available online at http://ieeexplore.ieee.org.

Digital Object Identifier 10.1109/TNNLS.2013.2286175

this problem domain [29]–[35], [38]–[48]. Fractional calculus has also been hybridized with artificial machine intelligence, mainly because of its inherent strength of long-term memory and non-locality. In the fields of fractional pattern recognition, adaptive control, and adaptive signal processing, fractional partial differential equations, based on the fractional Green formula and fractional Euler–Lagrange equation, must be implemented [46]–[48]. The fractional extreme points of the quadratic energy norm are quite different from the traditional integer-order extreme points such as the first-order stationary points. To determine the fractional extreme points of the quadratic energy norm, we propose generalizing the integer-order steepest descent method to the fractional-order one.

Unlike the classical FOSD method, the FAL approach has two distinct properties. First, the v-order fractional extreme points of the quadratic energy norm E are not coincident with the first-order extreme points of E. In this manner, the iterative search process of the FAL approach can easily pass over the first-order local extreme points of E. Second, if the fractional differential order of the FAL approach satisfies $0 < v < 1$, then the quadratic energy norm E has a single fractional extreme point or two asymmetric v-order fractional extreme points in a pair. The number of fractional extreme points depends on the value of v. To obtain a single fractional extreme point of E, v must be set to the appropriate value. If $1 < v < 2$, then the quadratic energy norm E has two asymmetric v-order fractional extreme points in a pair. This asymmetric characteristic is essential to the quadratic energy norm E and the property of nature. If $2 \leq k < v < k+1$, where k is a positive integer, the quadratic energy norm E has no fractional extreme point.

II. Related Works

This section includes a brief introduction to the basic definitions in the domain of fractional calculus. It is well known that fractal geometry generalizes the Newton–Leibniz derivative. Fractal theory modified the perspective of measure theory; in particular, Euclidean-measure-based fractional calculus is more developed than the Hausdorff-measure-based one. This is why the definition of fractional calculus based on the Euclidean measure is widely used. The commonly-used fractional calculus definitions are the Grünwald–Letnikov definition, Riemann–Liouville definition, and Caputo definition [12]–[15].

The Grünwald–Letnikov fractional calculus of order v is defined by

$$\begin{aligned} &D^v_{G-L}s(x) \\ &= \frac{d^v}{[d(x-a)]^v}s(x)\bigg|_{G-L} \\ &= \lim_{N\to\infty}\left\{\frac{\left(\frac{x-a}{N}\right)^{-v}}{\Gamma(-v)}\sum_{k=0}^{N-1}\frac{\Gamma(k-v)}{\Gamma(k+1)}s\left(x-k\left(\frac{x-a}{N}\right)\right)\right\} \end{aligned} \quad (1)$$

where $s(x)$ is the signal under consideration, $[a, x]$ is the duration of $s(x)$, v is a real number (can be fractional in nature too), and Γ is the Gamma function. Here, D^v_{G-L} denotes the Grünwald–Letnikov fractional differential operator. The Grünwald–Letnikov definition of fractional calculus is easy to calculate numerically; its numerical computation only requires the discrete sampling values, $s(x - k((x-a)/N))$, of signal $s(x)$. It only carries out the derivative or integral operation for the signal $s(x)$.

The Riemann–Liouville fractional integral of order v is defined by

$$\begin{aligned} D^v_{R-L}s(x) &= \frac{d^v}{[d(x-a)]^v}s(x)\bigg|_{R-L} \\ &= \frac{1}{\Gamma(-v)}\int_a^x (x-\eta)^{-v-1}s(\eta)d\eta \\ &= \frac{-1}{\Gamma(-v)}\int_a^x s(\eta)d(x-\eta)^{-v}, \quad v \prec 0 \end{aligned} \quad (2)$$

where D^v_{R-L} denotes the Riemann–Liouville fractional differential operator. The values of $v \geq 0$, and $0 \leq n-1 < v < n, n \in \boldsymbol{R}$ are fixed. The Riemann–Liouville fractional differential of order v is defined by

$$\begin{aligned} D^v_{R-L}s(x) &= \frac{d^v}{[d(x-a)]^v}s(x)\bigg|_{R-L} \\ &= \frac{d^n}{dx^n}\frac{d^{v-n}}{[d(x-a)]^{v-n}}s(x)\bigg|_{R-L} \\ &= \sum_{k=0}^{n-1}\frac{(x-a)^{k-v}s^{(k)}(a)}{\Gamma(k-v+1)} \\ &\quad + \frac{1}{\Gamma(n-v)}\int_a^x \frac{s^{(n)}(\eta)}{(x-\eta)^{v-n+1}}d\eta, \quad 0 \leq v \prec n. \end{aligned} \quad (3)$$

The definition of the Caputo fractional differential of order v is defined by

$${}^C_a D^v_x s(x) = \frac{1}{\Gamma(n-v)}\int_a^x (t-\tau)^{n-v-1}s^{(n)}(\tau)d\tau \quad (4)$$

where ${}^C_a D^v_x$ is the Caputo fractional differential operator. In this manner, the Fourier transform of signal $s(x)$ is defined by

$$\mathrm{FT}[D^v s(x)] = (i\omega)^v \mathrm{FT}[s(x)] - \sum_{k=0}^{n-1}(i\omega)^k \frac{d^{v-1-k}}{dx^{v-1-k}}s(0) \quad (5)$$

where i is the imaginary unit, and ω is the digital frequency. If $s(x)$ is a causal signal, (5) simplifies to $\mathrm{FT}[D^v s(x)] = (i\omega)^v \mathrm{FT}[s(x)]$.

III. Fractional Adaptive Learning Approach and Its Convergence

In this section, a FAL approach is proposed, which has been named as the fractional steepest descent approach and its convergence is described in detail. To better understand the difference between the FAL approach and the integer-order one, the first-order extreme value is taken into account to construct the quadratic energy norm, given as

$$E = E^1_{\min} + \eta(s^{1*} - s)^2 \quad (6)$$

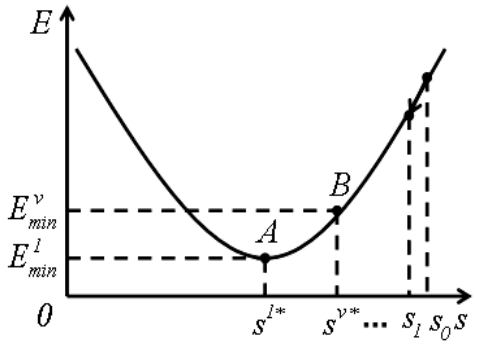

Fig. 1. Iterative search process of the FAL approach.

where $v > 0$, E is the quadratic energy norm, $\eta \neq 0$ is a constant that controls the degree of convexity-concavity, and $E^1_{\min}$ is the first-order extreme value of E. The performance curve of E is a parabola whose *a priori* knowledge is often unavailable. The reverse incremental search of the FAL approach is in the negative direction of the v-order fractional gradient of E, which can be given as

$$s_{k+1} = s_k + \mu(-D^v_{s_k}) \tag{7}$$

where k is the step size or number of iterations, s_k is the current adjusted value of s, s_{k+1} is the updated adjusted value of s, $D^v_{s_k}$ is the v-order fractional gradient of energy norm E at $s = s_k$, and μ is the constant coefficient that controls the stability and the rate of convergence of the FAL approach. Thus, the iterative search process of the FAL approach can be shown as given in Fig. 1.

As shown in Fig. 1, for the first-order extreme value $E^1_{\min}$, A is the first-order extreme point or stationary point of E, and s^{1*} is the first-order optimal value of s. In contrast, for the fractional extreme value $E^v_{\min}$, B is the v-order fractional extreme point or fractional stationary point of E, and s^{v*} is the fractional optimal value of s. s_0 is the initial value of s, selected at random.

From (1), it can be derived that $D^v_{x-a}[0] = 0$ and $D^v_{x-a}[c] = c((x-a)^{-v})/(\Gamma(1-v))$, where [0] denotes the permanent zero constant, and $[c]$ is a non-zero constant. Unlike the integer-order differentials, the fractional differential of a non-zero constant is equal to a non-zero value. Thus, the v-order fractional extreme point B is not coincident with the first-order extreme point A, and $E^v_{\min}$ is not the smallest value of E. If n and N are non-negative integers, $(\Gamma(-n)/\Gamma(-N)) = (-1)^{N-n}(N!/n!)$. From (1) and (7), and according to properties of fractional calculus, the following is true:

$$D^v_{s_k} = \left.\frac{d^v E}{ds^v}\right|_{s=s_k} = \frac{\left[E^1_{\min} + \eta(s^{1*})^2\right]s_k^{-v}}{\Gamma(1-v)} - \frac{2\eta s^{1*} s_k^{1-v}}{\Gamma(2-v)} + \frac{2\eta s_k^{2-v}}{\Gamma(3-v)}. \tag{8}$$

Equation (8) shows that $D^v_{s_k}$ is a nonlinear equation of s_k, involving non-constant coefficients. It is quite difficult to directly derive the analytical expression of $D^v_{s_k}$ using v as a variable. Fortunately, if the order v of the FAL approach is known or specified, the formula described in (8) gets transformed to a constant coefficient nonlinear equation. When the iterative search process of the FAL approach converges to a stable solution, $s_{k+1} = s_k = s^{v*}$, $D^v_{s_k} = 0$, and $E = E^v_{\min}$. Thus, from (6) and (8), the following can be obtained:

$$E^v_{\min} = E^1_{\min} + \eta(s^{1*})^2 - 2\eta s^{1*}s^{v*} + \eta(s^{v*})^2 \tag{9}$$

$$(s^{v*})^{-v}\left\{\frac{E^1_{\min} + \eta(s^{1*})^2}{\Gamma(1-v)} - \frac{2\eta s^{1*}}{\Gamma(2-v)}s^{v*} + \frac{2\eta}{\Gamma(3-v)}(s^{v*})^2\right\} = 0. \tag{10}$$

From (10), we conclude that $s^{v*} \neq 0$. Thus, (10) can be simplified as a constant coefficient quadratic equation, given as

$$\frac{E^1_{\min} + \eta(s^{1*})^2}{\Gamma(1-v)} - \frac{2\eta s^{1*}}{\Gamma(2-v)}s^{v*} + \frac{2\eta}{\Gamma(3-v)}(s^{v*})^2 = 0. \tag{11}$$

From (11), we can derive the relationship between s^{v*} and s^{1*}

$$s^{v*}_{1,2} = \frac{\Gamma(3-v)}{2\eta} \times \left\{\frac{\eta s^{1*}}{\Gamma(2-v)} \pm \sqrt{\frac{\eta^2(s^{1*})^2}{\Gamma^2(2-v)} - \frac{2\eta\left[E^1_{\min} + \eta(s^{1*})^2\right]}{\Gamma(1-v)\Gamma(3-v)}}\right\}. \tag{12}$$

Equation (12) implies that the v-order fractional extreme points of E are not always unique; however, they always appear as a pair of points. In general, the v-order fractional extreme points of E in a pair are asymmetric about s^{1*}. If (12) has two different solutions, the FAL approach will converge to either s^{v*}_1 or s^{v*}_2, respectively. Fig. 1 and (12) show that the convergence value (s^{v*}_1 or s^{v*}_2) of the iterative search process is related to the initial value s_0, selected at random. If (12) has two different solutions, the FAL approach is difficult to control and does not converge to the expected stable point. Hence, in order to ensure the convergence to a single v-order fractional extreme point, the two solutions in (12) must be equal, i.e., $s^{v*} = s^{v*}_1 = s^{v*}_2$. Let us make $s^{v*} \neq 0$. Then, according to the properties of the Gamma function, it can be derived that $1/(\Gamma(1-v)\Gamma(3-v)) = 0$, if $v = 1, 3$, and $1/(\Gamma(2-v)) = 0$, if $v = 2$. Thus, from (12), the relationship between a single fractional optimal value s^{v*} and the first-order optimal value s^{1*} can be derived as

$$s^{v*} = \frac{\Gamma(3-v)s^{1*}}{\Gamma(2-v)} \overset{v=1}{=} s^{1*}, \quad \text{if } v = 1, 3, \text{ and } v \neq 2. \tag{13}$$

Equation (13) shows that the classical FOSD method is a special case of the FAL approach (called fractional steepest descent approach). When $v \neq 1, 2, 3$ and

$$\frac{\eta^2(s^{1*})^2}{\Gamma^2(2-v)} - \frac{2\eta\left[E^1_{\min} + \eta(s^{1*})^2\right]}{\Gamma(1-v)\Gamma(3-v)} = 0$$

(12) has a unique solution $s^{v*} = s^{v*}_1 = s^{v*}_2$, and E has a single v-order fractional extreme point. Note that the v-order FAL approach must satisfy

$$\frac{\Gamma(1-v)\Gamma(3-v)}{\Gamma^2(2-v)} = \frac{2E^1_{\min}}{\eta(s^{1*})^2} + 2, \quad \text{if } v \neq 1, 2, 3. \tag{14}$$

Substituting (14) into (12), the relationship between s^{v*} and s^{1*} can be derived as

$$s^{v*} = \frac{\Gamma(3-v)s^{1*}}{2\Gamma(2-v)}, \quad \text{if } v \neq 1, 2, 3. \tag{15}$$

In this equation, if $v \neq 1, 2, 3$ and v satisfies (14), the convergence value of the iterative search process of the FAL approach is s^{v*}. Thus, substituting (9) and (15) into (6), the energy norm E, expressed in terms of the fractional extreme value $E^v_{\min}$ and fractional optimal value s^{v*}, can be derived as

$$E = E^v_{\min} + \eta \left[\frac{4\Gamma(2-v) - \Gamma(3-v)}{\Gamma(3-v)} (s^{v*})^2 - \frac{4\Gamma(2-v)}{\Gamma(3-v)} s^{v*} s + s^2 \right]. \quad (16)$$

Substituting (8) into (7), the transient property of the iterative search process can be derived from s_0 to s^{v*}, for this FAL approach, given as

$$s_{k+1} = s_k - \frac{\mu \left[E^1_{\min} + \eta (s^{1*})^2 \right] s_k^{-v}}{\Gamma(1-v)} + \frac{2\mu\eta s^{1*} s_k^{1-v}}{\Gamma(2-v)} - \frac{2\mu\eta s_k^{2-v}}{\Gamma(3-v)}. \quad (17)$$

Substituting (11) into (17), one can obtain

$$s_{k+1} = s_k - \frac{2\mu\eta}{\Gamma(3-v)} \left[s_k^2 - \frac{\Gamma(3-v)}{\Gamma(2-v)} s^{1*} s_k - (s^{v*})^2 + \frac{\Gamma(3-v)}{\Gamma(2-v)} s^{1*} s^{v*} \right] s_k^{-v}. \quad (18)$$

Then, substitution of (15) into (18) results in

$$s_{k+1} = s_k - \frac{2\mu\eta}{\Gamma(3-v)} (s_k - s^{v*})^2 s_k^{-v}, \quad \text{if } v \neq 1, 2, 3. \quad (19)$$

Equation (19) shows that it is a nonlinear, non-constant coefficient, difference equation. It is not possible to directly derive the general term of s_k by mathematical induction. To simplify this nonlinear calculation, let us consider s_k as a discrete sampling of the continuous function $s(t)$ about t. Then, the first-order difference can be used as an approximation for the first-order differential. It means $D^1_t s(t) \cong s_{k+1} - s_k$. In addition, the power series expansion of s^v about $(s - s^{v*})$ can also be derived. It can be given as

$$s^v = \sum_{n=0}^{\infty} \frac{\Gamma(1+v)(s^{v*})^{v-n}(s - s^{v*})^n}{\Gamma(n+1)\Gamma(1-n+v)}.$$

To further simplify this nonlinear computation, we only take the item summation of the power series expansion of s^v, when $n = 0$ and $n = 1$, as the approximation of s^v. One can then derive that $s^v \cong v(s^{v*})^{v-1} s$. Thus, (19) can be rewritten as

$$D^1_t s(t) \cong \frac{-2\mu\eta}{\Gamma(3-v)v(s^{v*})^{v-1} s(t)} [s(t) - s^{v*}]^2, \quad \text{if } v \neq 1, 2, 3. \quad (20)$$

Equation (20) is a first-order ordinary differential equation with variables that are separable. Solving (20) by separation of variables, one can arrive at the solution $s(t)$. By discretely sampling $s(t)$ about t, the general form of s_k can be obtained

$$s_k \cong s^{v*} + \exp\left(\frac{-2\mu\eta k}{\Gamma(3-v)v(s^{v*})^{v-1}} \right), \quad \text{if } v \neq 1, 2, 3. \quad (21)$$

For the iterative search process of the FAL approach to converge, it must meet the condition

$$\lim_{k \to +\infty} \frac{2\mu\eta k}{\Gamma(3-v)v(s^{v*})^{v-1}} = +\infty$$

which implies

$$\frac{2\mu\eta}{\Gamma(3-v)v(s^{v*})^{v-1}} = \chi > 0$$

where χ is a positive constant. Thus, the constant coefficient μ satisfies

$$\mu \cong \frac{\chi\Gamma(3-v)v(s^{v*})^{v-1}}{2\eta}, \quad \text{if } v \neq 1, 2, 3. \quad (22)$$

Variables s_k and k of the classical FOSD method are related by a geometric series [49]. The iterative search process of the FOSD method can be classified as three categories: 1) overdamped oscillation; 2) critically damped oscillation; and 3) underdamped oscillation [49]. Unlike the FOSD method, (21) shows that the relationship between s_k and k of the FAL approach is an approximate negative power geometric series. First, when $\chi = 1$

$$\mu \cong \frac{\Gamma(3-v)v(s^{v*})^{v-1}}{2\eta}, \quad \text{if } v \neq 1, 2, 3.$$

Substituting this approximation into (21) yields

$$s_k \cong s^{v*} + \exp(-k), \quad \text{if } v \neq 1, 2, 3.$$

Thus, when $\chi = 1$, the iterative search process of the FAL approach converges in the form of $\exp(-k)$. Second, when $\chi = 2$

$$\mu \cong \frac{\Gamma(3-v)v(s^{v*})^{v-1}}{\eta}, \quad \text{if } v \neq 1.$$

Substituting this approximation into (21) yields

$$s_k \cong s^{v*} + \exp(-2k), \quad \text{if } v \neq 1, 2, 3.$$

Thus, when $\chi = 2$, the iterative search process of the FAL approach converges rapidly in the form of $\exp(-2k)$. Third, when χ is an integer and $\chi \geq 3$, the iterative search process of the FAL approach converges sharply in the form of $\exp(-\chi k)$. Similarly, when $n - 1 < \chi = v < n$, the iterative search process of the FAL approach converges rapidly in the form of $\exp(-vk)$. In general, the FAL approach on multi-dimensional performance surface of the quadratic energy norm is a generalization of (6). Equation (6) shows that the energy norm and reverse incremental search process of the multi-dimensional FAL approach are equivalent to $\boldsymbol{E} = \boldsymbol{E}^1_{\min} + \boldsymbol{\eta}(\boldsymbol{s}^{1*} - \boldsymbol{s})^2$ and $\boldsymbol{s}_{k+1} = \boldsymbol{s}_k + \boldsymbol{\mu}(-\boldsymbol{D}^v_{\boldsymbol{s}_k})$, respectively, where the constant coefficients $\boldsymbol{\eta}$ and $\boldsymbol{\mu}$ are multi-dimensional vectors. Here $\boldsymbol{\mu}$ satisfies the condition, given as

$$\boldsymbol{\mu} \cong \left\{ \frac{\chi\Gamma(3-v)v(\boldsymbol{s}^{v*})^{v-1}}{2\boldsymbol{\eta}} \right\}, \quad \text{if } v \neq 1, 2, 3. \quad (23)$$

IV. Experiments and Analysis

A. Application of the Fractional Adaptive Learning Approach

This section briefly describes the application of the FAL approach. In view of signal processing applications, the fractional differential has the following nonlinear characteristics [34], [42], [44], [45]. First, the fractional differential of a non-zero constant is not equal to zero. It decreases gradually to zero from the highest value on

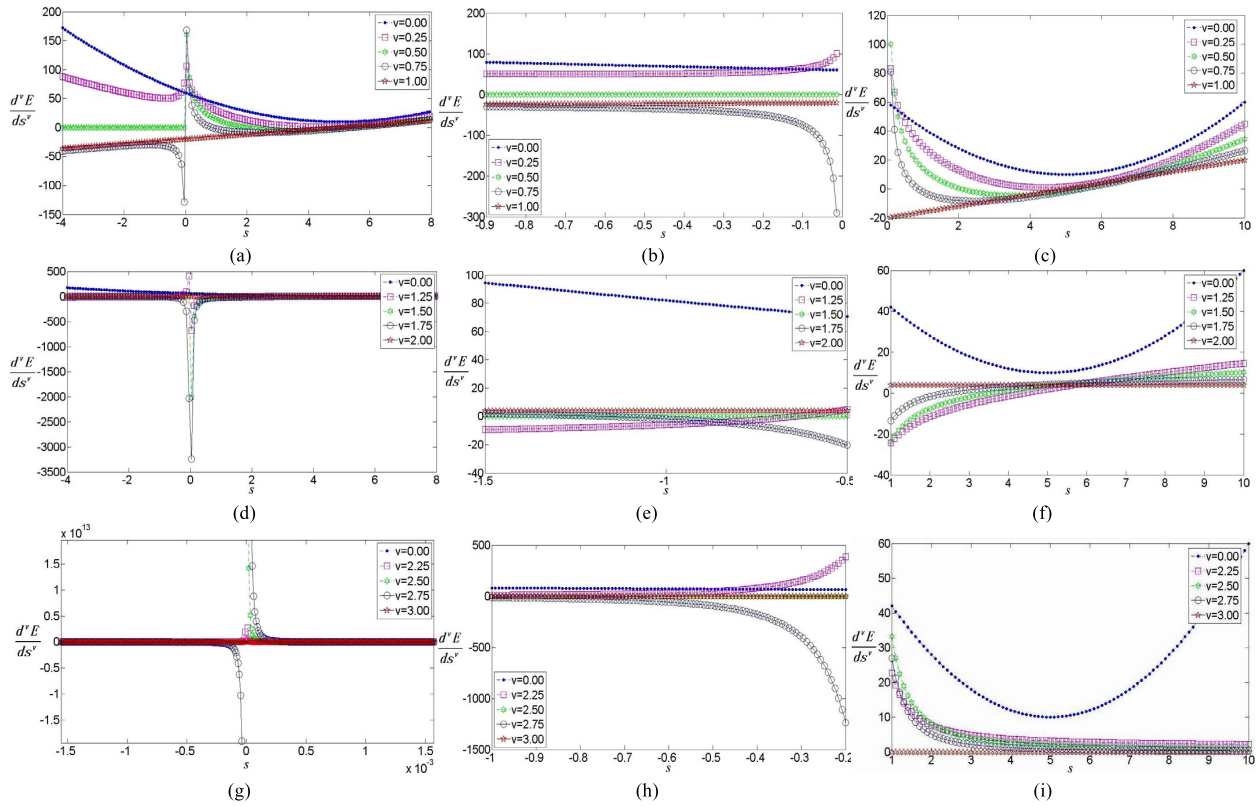

Fig. 2. v-order fractional differential of the energy norm E. (a) $0 \le v \le 1$. (b) Partial enlarged details when $-0.9 < s < 0$ and $0 \le v \le 1$. (c) Partial enlarged details when $0 < s < 10$ and $0 \le v \le 1$. (d) $1 < v \le 2$. (e) Partial enlarged details when $-1.5 < s < -0.5$ and $1 < v \le 2$. (f) Partial enlarged details when $1 < s < 10$ and $1 < v \le 2$. (g) $2 < v \le 3$. (h) Partial enlarged details when $-1 < s < -0.2$ and $2 < v \le 3$. (i) Partial enlarged details when $1 < s < 10$ and $2 < v \le 3$.

a singular impulse signal. In contrast, any integer-order differential of a constant is equal to zero. This is a remarkable difference between the fractional differential and the integer-order differential. Second, the fractional differential at the initial point of a ramp function is equal to non-zero, which nonlinearly enhances the high-frequency singular information. If $v = 1$ or $v = 2$, the classical Sobel operator and Gaussian operator coincide with the first-order and second-order differential operators, respectively. In contrast, if $0 < v < 1$, the fractional differential enhancement of high-frequency singular information is smaller than its first-order differential enhancement; moreover, when the order of the fractional differential increases, the enhancement of high-frequency singular information also increases. Third, the fractional differential of a ramp function does not possess a linear relation; instead, it yields a nonlinear curve. In contrast, the integer-order differential of a ramp function does possess a linear relation.

Based on the aforementioned nonlinear characteristics of the fractional differential, the FAL approach can be applied to the image processing problems [34], [42], [44]–[48]. The fractional differential has been demonstrated to preserve, in great detail, the low-frequency contour features in smooth areas. It also enhances the high-frequency marginal information in highly variable greyscale areas and enhances the texture details in areas where greyscale changes are not as obvious. All of this is done in a nonlinear fashion. As such, the FAL approach can be used to perform reverse incremental optimizing searches on the fractional total variation in an image. By using the FAL approach, we can implement a class of multi-scale denoising models for texture images based on the nonlinear fractional partial differential equations that preserve texture details. In this case, the desired objective is achieved in a non-linear fashion [46]–[48].

B. Stability and Convergence of the Fractional Adaptive Learning Approach

In this section, the stability and convergence of the FAL approach are discussed. The properties of the v-order fractional differential of the energy norm E are analyzed using fractional calculus. Without loss of generality, we set $E^1_{\min} = 10$, $\eta = 2$, and $s^{1*} = 5$ in (6) and (8). Then, as shown in Fig. 2, we numerically implement the v-order derivative

$$D^v_s = \frac{d^v E}{ds^v} = \frac{\left[E^1_{\min} + \eta(s^{1*})^2\right]s^{-v}}{\Gamma(1-v)} - \frac{2\eta s^{1*}s^{1-v}}{\Gamma(2-v)} + \frac{2\eta s^{2-v}}{\Gamma(3-v)}$$

of the energy norm $E = E^1_{\min} + \eta(s^{1*} - s)^2$ about s.

As shown in Fig. 2, if $v = 0$, D^v_s performs neither the differential nor the integral operations. If $v > 0$, D^v_s performs the fractional differential operation. In Fig. 2(a), (d), and (g), for

$$D^v_s = \frac{d^v E}{ds^v} = \frac{\left[E^1_{\min} + \eta(s^{1*})^2\right]s^{-v}}{\Gamma(1-v)} - \frac{2\eta s^{1*}s^{1-v}}{\Gamma(2-v)} + \frac{2\eta s^{2-v}}{\Gamma(3-v)}$$

the v-order fractional calculus has two obvious undermentioned features. First, the v-order fractional calculus of most functions is equal to a power function. Second, the v-order fractional calculus of the remaining functions is equal to the

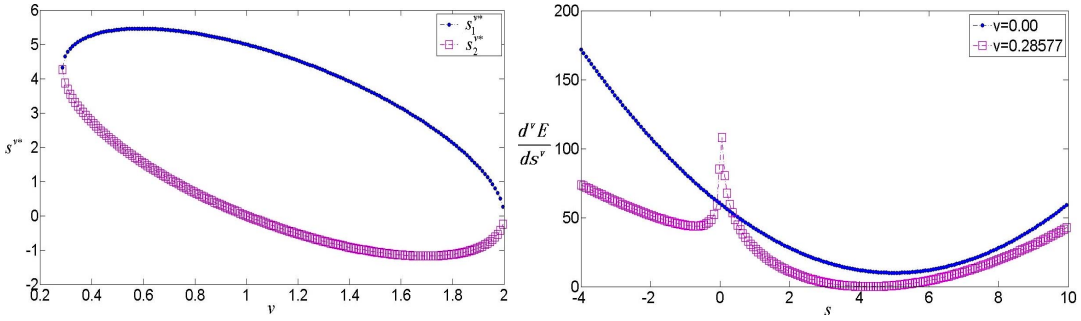

Fig. 3. Relationship between s_1^{v*} and s_2^{v*} and the $v \cong 0.28577$ order fractional derivative of E. (a) Relationship between s_1^{v*} and s_2^{v*}. (b) $v \cong 0.28577$ order fractional derivative of E.

sum or product of a certain functions and power function. In this way, the v-order fractional calculus may go on ad infinitum if the denominator of the power function is equal to zero. Therefore, in Fig. 2(a), (d), and (g), if $s = 0$, d^vE/ds^v has a singular impulse. Fig. 2(a) and (b) also show that if $s < 0$, $0 < v < 1$, and $v \neq (1/2)$, (d^vE/ds^v) has a non-zero crossing point. If $s < 0$ and $v = 1/2$, $(d^vE/ds^v) \equiv 0$. Equation (14) shows that when v_z satisfies

$$\frac{\Gamma(1-v_z)\Gamma(3-v_z)}{\Gamma^2(2-v_z)} = \frac{2E^1_{\min}}{\eta(s^{1*})^2} + 2, \quad \text{if } v_z \neq 1$$

(12) has two identical solutions. There is a single fractional optimal value $s^{v*} = s_1^{v*} = s_2^{v*}$ when the value of v_z is related to $E^1_{\min}$, η, and s^{1*}. As shown in Fig. 2(a) and (c), if $0 < v < v_z < 1$, (d^vE/ds^v) has a non-zero crossing point. If $0 < v = v_z < 1$, $D_s^v = (d^vE/ds^v)$ has a single zero crossing point, and if $0 < v_z < v < 1$, it has two zero crossing points. In other words, if $0 < v < 1$, there may not be a single fractional extreme point of E; in general, the v-order fractional extreme points of E occur in pairs, which are asymmetric about s^{1*}. This suggests that if $E^1_{\min}$, s^{1*}, and η are arbitrary, the v-order fractional extreme value s^{v*} of E exists either individually or as a pair. Fig. 2(a)–(c) show that if $v = 1$, $D_s^v = (d^vE/ds^v)$ has a single zero crossing point. As shown in Fig. 2(d)–(f), if $1 < v < 2$, $D_s^v = (d^vE/ds^v)$ has a pair of zero crossing points asymmetrical about s^{1*}. If $v = 2$, $D_s^v = (d^vE/ds^v) = \eta = 2 \neq 0$. As shown in Fig. 2(g)–(i), if $2 < v < 3$, $D_s^v = (d^vE/ds^v)$ has a non-zero crossing point. If $v = 3$, $D_s^v = (d^vE/ds^v) \equiv 0$. Therefore, if $2 \leq k < v < k+1$, $D_s^v = (d^vE/ds^v)$ has a non-zero crossing point. If $v = k+1$, $D_s^v = (d^vE/ds^v) \equiv 0$.

Furthermore, from (14), we can further conclude that if $E^1_{\min} = 10$, $\eta = 2 \neq 0$, and $s^{1*} = 5$, the solution of

$$\frac{\Gamma(1-v)\Gamma(3-v)}{\Gamma^2(2-v)} = \frac{2E^1_{\min}}{\eta(s^{1*})^2} + 2, \quad \text{if } v \neq 1$$

is equal to $v \cong 0.28577$, which shows that E has a single v-order fractional extreme value. Thus, from (8), (12), and (14), we can numerically implement s_1^{v*}, s_2^{v*}, and the $v \cong 0.28577$ order fractional derivative of E. It is shown in Fig. 3.

From Fig. 3(a), note that if $v \cong 0.28577$, (12) has two identical solutions, and there is a single fractional optimal value $s^{v*} = s_1^{v*} = s_2^{v*}$ of E. From Fig. 3(b), if $v \cong 0.28577$, $D_s^v = (d^vE/ds^v)$ has a single zero crossing point of E. The experiment results obtained coincide with the aforementioned theoretical derivation.

Recall that the v-order fractional extreme point of E is not coincident with the first-order extreme point of E. This implies that the iterative search process of the FAL approach easily passes over the first-order local extreme points of E. From (14), if v_z satisfies

$$\frac{\Gamma(1-v_z)\Gamma(3-v_z)}{\Gamma^2(2-v_z)} = \frac{2E^1_{\min}}{\eta(s^{1*})^2} + 2, \quad \text{if } v_z \neq 1$$

(12) has two identical solutions, and there is a single fractional optimal value

$$s^{v*} = \frac{\Gamma(3-v)s^{1*}}{2\Gamma(2-v)}, \quad \text{if } v \neq 1.$$

Furthermore, if $0 < v_z < v < 1$, (12) has two different solutions; specifically

$$s_{1,2}^{v*} = \frac{\Gamma(3-v)}{2\eta} \times \left\{ \frac{\eta s^{1*}}{\Gamma(2-v)} \pm \sqrt{\frac{\eta^2(s^{1*})^2}{\Gamma^2(2-v)} - \frac{2\eta\left[E^1_{\min} + \eta(s^{1*})^2\right]}{\Gamma(1-v)\Gamma(3-v)}} \right\}.$$

The v-order fractional extreme points of E occur in pairs that are asymmetrical about s^{1*}.

We also consider the stability and convergence rate of the FAL approach. If (12) has two different solutions, the FAL approach will converge to s_1^{v*} or s_2^{v*}. The convergence value (s_1^{v*} or s_2^{v*}) of its iterative search process is related to the randomly selected initial value s_0. In Fig. 2(d)–(f), $v = 1.25$ serves as an example for discussion. Equation (12) shows that when the iterative search process of the FAL approach converges to a steady state, then $s_{k+1} = s_k = s^{v*}$, $D_{s_k}^v = 0$, and $E = E^v_{\min}$. Specifically, we determined $s_1^{v*} = 4.3906$ and $s_2^{v*} = -0.6406$. For numerical implementation, Let us set $\mu = 0.005$, the total number of iterations $k = 500$, and the initial values $s_{10} = 4.5$ and $s_{20} = -0.25$. From (17), we implement the iterative search process of the FAL approach in 1-D space, as shown in Fig. 4.

As shown in Fig. 4, when the iterative search process of the FAL approach converges to a steady state, $s_{1k} = 4.3906 = s_1^{v*}$ and $s_{2k} = -0.6406 = s_2^{v*}$. The reverse incremental search of the FAL approach is in the negative direction of the v-order fractional gradient of E. Thus, if μ is set to an appropriate

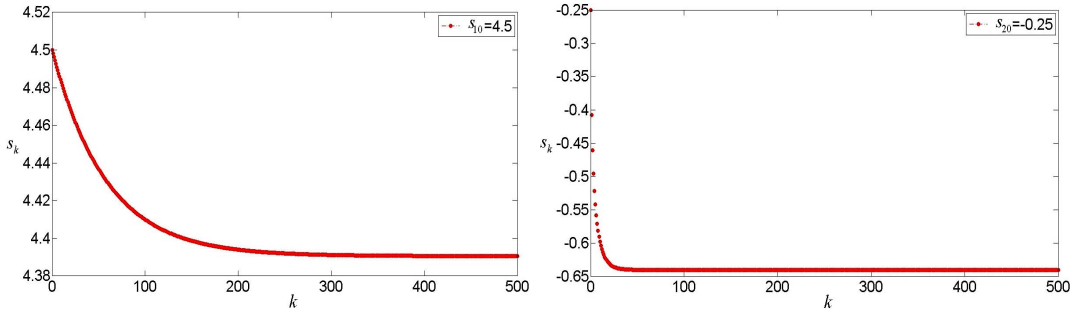

Fig. 4. Randomly selected initial value s_0 and the final convergence value of the FAL approach when (a) $s_{10} = 4.5$, and (b) $s_{20} = -0.25$.

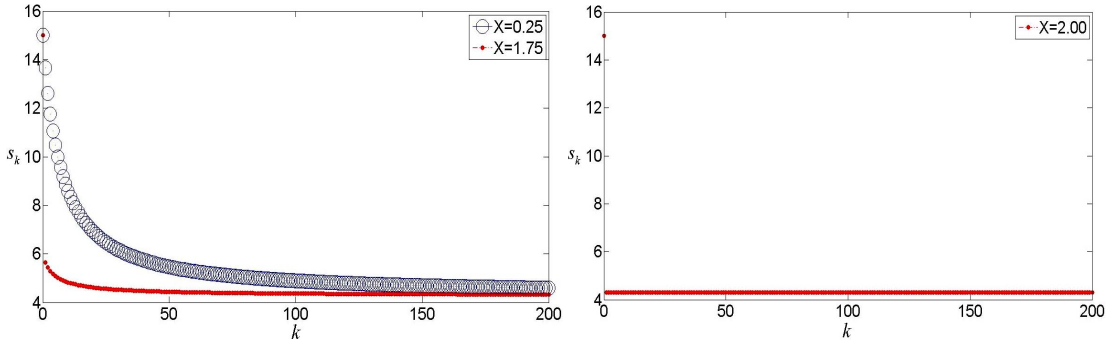

Fig. 5. Iterative search process of the FAL approach in 1-D space when (a) $0 < \chi = 0.25 < 2$ and $0 < \chi = 1.75 < 2$, and (b) $\chi = 2.00$.

value, its iterative search process will stop when $D^v_{s_k} = 0$ and converge to the $v = 1.25$ order fractional extreme point of E. The results in Fig. 2(d)–(f) conform to the theoretical derivations achieved in (7), (12), and (17), respectively. Thus, in order to converge to a single v-order fractional extreme point, the two solutions of (12) must be identical, i.e., there is a single fractional optimal value $s^{v*} = s_1^{v*} = s_2^{v*}$.

If (14) is satisfied, (12) has two identical solutions $s^{v*} = s_1^{v*} = s_2^{v*}$. From (14), when $v \cong 0.28577$, it has a single v-order fractional extreme point of E. Thus, from (9) and (15), we derive

$$s^{v*} = \frac{\Gamma(3-v)s^{1*}}{2\Gamma(2-v)} \overset{v\cong 0.28577}{\cong} 4.2856$$
$$E^v_{\min} = E^1_{\min} + \eta(s^{1*})^2 - 2\eta s^{1*}s^{v*} + \eta(s^{v*})^2 \cong 11.0208.$$

For (19), the randomly selected initial value $s_0 = 15$, and the total number of iterations is 200. Furthermore, It is also assumed that $0 < \chi = 0.25 < 2$, $0 < \chi = 1.75 < 2$, and $\chi = 2$ in (22). Equations (19) and (22) are implemented numerically using the iterative search process of the FAL approach in 1-D space, as shown in Fig. 5.

As shown in Fig. 5 and (21), if $0 < \chi = 0.25 < 2$, $\mu = 0.0099$. The iterative search process of the FAL approach converges in the exponential form of $\exp(-0.25k)$ that depicts that its iterative search process is slower in nature. When $k = 200$, the search process converges to the stable state $s_k = 4.3270$. On the other hand, if $0 < \chi = 1.75 < 2$, $\mu = 0.0691$. The iterative search process of the FAL approach converges in the exponential form of $\exp(-1.75k)$. As χ and μ increase, the iterative search process is accelerated. When $k = 50$, the search process converges to the stable state of $s_k = 4.3270$. Furthermore, if $\chi = 2$, $\mu = 0.0790$. The iterative search process of the FAL approach converges in the exponential form of $\exp(-2k)$ which depicts that its iterative search process is very fast. When $k = 1$, it converges to the stable state of $s_k = 4.2945$, only in a single one step. Note that to simplify the nonlinear calculation in (20), only the item summation of the power series expansion of s^v needs to be considered when $n = 0$ and $n = 1$. This approximation leads to a small deviation. The three extreme values of the aforementioned experiments are approximate to $s_k \cong s^{v*}$, respectively.

Next, the stability and convergence rate of the FAL approach in high-dimensional space are examined in depth. In 3-D space, we assume ${}_xE^1_{\min} = 10$, $\eta_x = 2 \neq 0$, $s_x^{1*} = 5$, ${}_yE^1_{\min} = {}_xE^1_{\min} = E^1_{\min}$, $\eta_y = 3 \neq 0$ and $s_y^{1*} = 6$. Consequently, $E = E^1_{\min} + \eta_x(s_x^{1*} - s_x)^2 + \eta_y(s_y^{1*} - s_y)^2$. As shown in (14), when $v_x \cong 0.28577$, $\boldsymbol{E}$ has a single v_x-order fractional extreme point in the x coordinate direction. Likewise, when $v_y \cong 0.15625$, $\boldsymbol{E}$ has a single v_y-order fractional extreme value in the y coordinate direction. From (9) and (15), it follows that:

$$s_x^{v*} = \frac{\Gamma(3-v_x)s_x^{1*}}{2\Gamma(2-v_x)} \overset{v_x\cong 0.28577}{\cong} 4.2856$$
$${}_xE^v_{\min} = {}_xE^1_{\min} + \eta_x\left(s_x^{1*}\right)^2 - 2\eta_x s_x^{1*}s_x^{v*} + \eta_x\left(s_x^{v*}\right)^2 \cong 11.0208$$
$$s_y^{v*} = \frac{\Gamma(3-v_y)s_y^{1*}}{2\Gamma(2-v_y)} \overset{v_y\cong 0.15625}{\cong} 5.5313$$
$${}_yE^v_{\min} = {}_yE^1_{\min} + \eta_y\left(s_y^{1*}\right)^2 - 2\eta_y s_y^{1*}s_y^{v*} + \eta_y\left(s_y^{v*}\right)^2 \cong 10.6592.$$

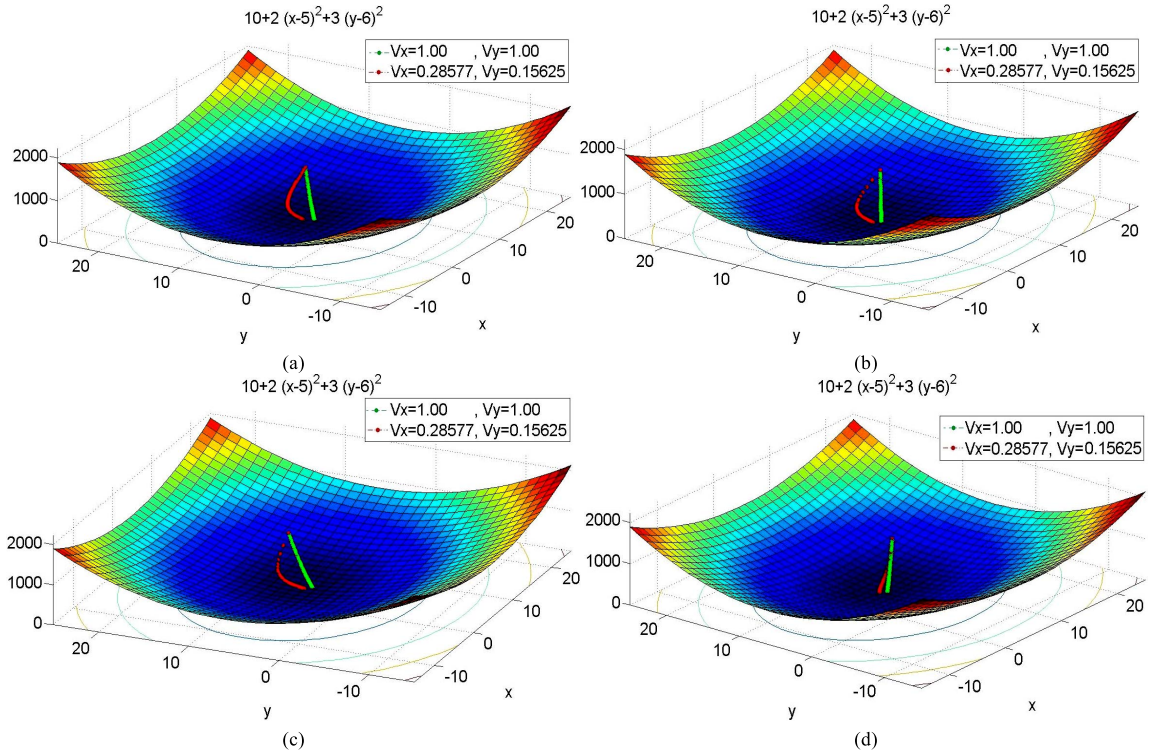

Fig. 6. Comparison of the iterative search process of the FAL approach and classical FOSD method in 3-D space when (a) $\chi = 0.25$ and $\boldsymbol{\mu} = \{\mu_x, \mu_y\}^{\chi=0.25} = \{0.0099, 0.0027\}$, (b) $\chi = 1.75$ and $\boldsymbol{\mu} = \{\mu_x, \mu_y\}^{\chi=1.75} = \{0.0691, 0.0187\}$, (c) $\chi = 2.00$ and $\boldsymbol{\mu} = \{\mu_x, \mu_y\}^{\chi=2} = \{0.0790, 0.0214\}$, (d) $\chi = 1.75$ and $\boldsymbol{\mu} = \max\{\mu_x, \mu_y\}^{\chi=1.75} = \{0.0691, 0.0691\}$.

In (19), the randomly selected initial values are ${}_xs_0 = 15$ and ${}_ys_0 = 12$. In (22) and (23), we fix the total number of iterations $k = 4000$, and set $\chi = 0.25$, $\chi = 1.75$, and $\chi = 2$. Thus, we determine $\boldsymbol{\mu} = \{\mu_x, \mu_y\}^{\chi=0.25} = \{0.0099, 0.0027\}$, $\boldsymbol{\mu} = \{\mu_x, \mu_y\}^{\chi=1.75} = \{0.0691, 0.0187\}$, $\boldsymbol{\mu} = \{\mu_x, \mu_y\}^{\chi=2} = \{0.0790, 0.0214\}$, and $\boldsymbol{\mu} = \max\{\mu_x, \mu_y\}^{\chi=1.75} = \{0.0691, 0.0691\}$. In (7) and (17), we set ${}_xs_0 = 15$, ${}_ys_0 = 12$, $v = 1$, $\mu_x = \mu_y = 0.01$, and $k = 250$. These values are used to implement the 3-D iterative search process of the FAL approach, as shown in Fig. 6.

As shown in Fig. 6(a), if $\chi = 0.25$ and $\boldsymbol{\mu} = \{\mu_x, \mu_y\}^{\chi=0.25} = \{0.0099, 0.0027\}$, the iterative search process of the FAL approach converges to $({}_xs_k, {}_ys_k) = (4.3137, 5.6221) \cong (s_x^{v*}, s_y^{v*})$. In Fig. 6(b), if $\chi = 1.75$ and $\boldsymbol{\mu} = \{\mu_x, \mu_y\}^{\chi=1.75} = \{0.0691, 0.0187\}$, the iterative search process converges to $({}_xs_k, {}_ys_k) = (4.2859, 5.5437) \cong (s_x^{v*}, s_y^{v*})$. Similarly, in Fig. 6(c), if $\chi = 2.00$ and $\boldsymbol{\mu} = \{\mu_x, \mu_y\}^{\chi=2} = \{0.0790, 0.0214\}$, the iterative search process of the FAL approach converges to $({}_xs_k, {}_ys_k) = (4.2890, 5.5421) \cong (s_x^{v*}, s_y^{v*})$. Finally, as shown in Fig. 6(d), if $\chi = 1.75$ and $\mu = \max\{\mu_x, \mu_y\}^{\chi=1.75} = \{0.0691, 0.0691\}$, the iterative search process converges to $({}_xs_k, {}_ys_k) = (4.2895, 5.5346) \cong (s_x^{v*}, s_y^{v*})$. These results suggest that if $\boldsymbol{\chi}$ and $\boldsymbol{\mu} = \{\mu_x, \mu_y\}$ are different values, the FAL approach converges simultaneously in the x and y coordinate directions.

Note that the nature of the curve surface of quadratic energy norm looks quite similar to a bowl in 3-D space. The FAL approach does not converge to the bottom of the bowl of the quadratic energy norm E. The larger the value of χ is, the faster is the convergence rate of FAL approach, and, the sparser is its convergence trajectory. As shown in Fig. 6(a)–(c), for $\mu_x \neq \mu_y$, the convergence rates in the x and y coordinate directions also vary; the convergence trajectory of the FAL approach is a nonlinear curve. Fig. 6(d) shows that for $\mu_x = \mu_y$, the convergence rates in the x and y coordinate directions are equal; the convergence trajectory of the FAL approach is a straight line. As shown in Fig. 6(a)–(d), the iterative search process of the classical FOSD method converges to $({}_xs_k, {}_ys_k) = (5.0004, 5.0003) \cong (s_x^{1*}, s_y^{1*})$. The classical FOSD method does converge to the bottom bowl of the quadratic energy norm E. As shown in Fig. 6, for $(s_x^{v*}, s_y^{v*}) \neq (s_x^{1*}, s_y^{1*})$, there is a small deviation between (s_x^{v*}, s_y^{v*}) and (s_x^{1*}, s_y^{1*}).

V. Conclusion

In recent times, the notion of how to apply fractional calculus to perform signal processing, and for the purpose of adaptive learning, has become a potent, emerging research problem and a few research studies have been initiated and reported all over the world. In the fields of fractional pattern recognition, adaptive control, and adaptive signal processing, fractional partial differential equations based on the fractional Green formula and fractional Euler–Lagrange equation have been implemented. The fractional extreme point of the quadratic energy norm is quite different from the traditional integer-order one such as the first-order

stationary point. To identify the fractional extreme points of the quadratic energy norm, we generalized the integer-order steepest descent method to a fractional approach. Based on the characteristics of fractional calculus mentioned above, a novel mathematical method is proposed where fractional calculus is used to implement FAL approach, named as fractional steepest descent approach.

Unlike the classical FOSD method, the FAL approach has two different properties. First, the v-order fractional extreme point of quadratic energy norm E is not coincident with the first-order extreme point of E. This means $E^v_{\min}$ is not the smallest value of E. In this manner, the iterative search process of the FAL approach can easily pass over the first-order local extreme points of E. Second, if the fractional differential order of the FAL approach satisfies $0 < v < 1$, the quadratic energy norm E may have a single fractional extreme point, or two asymmetric fractional extreme points in a pair about s^{1*}. The number of fractional extreme points depends on the value of order v. In order to achieve a single fractional extreme point of E, v must be set to an appropriate value. If $1 < v < 2$, the quadratic energy norm E always has two asymmetric v-order fractional extreme points in a pair about s^{1*}. This shows that the asymmetric characteristic is an essential property of the quadratic energy norm E and is also an essential property of nature. If $2 \leq k < v < k+1$, where k is a positive integer, the quadratic energy norm E has no fractional extreme point. For $(s_x^{v*}, s_y^{v*}) \neq (s_x^{1*}, s_y^{1*})$, there is a small deviation between (s_x^{v*}, s_y^{v*}) and (s_x^{1*}, s_y^{1*}).

The FAL approach can be suitably applied to implement textural image denoising [46]–[48]. It is well-known that the classical first-order Hopfield neural networks are based on the first-order differential and first-order adaptive learning approach, specifically the FOSD method. Thus, the FAL approach can also be applied to implement fractional Hopfield neural networks and anti-chip cloning attacks for anti-counterfeiting. Some initial discussions in these aspects are presented in [50] and [51]. It is intended that in-depth studies in these directions will be undertaken as future course of work.

REFERENCES

[1] S. Haykin, *Adaptive Filter Theory*. Englewood Cliffs, NJ, USA: Prentice-Hall, 2002.

[2] T. S. Alexander, *Adaptive Signal Processing: Theory and Applications*. New York, NY, USA: Springer-Verlag, 1986.

[3] M. G. Belfiore, *Adaptive Filters and Signal Analysis*. New York, NY, USA: Dekker, 1988.

[4] P. S. R. Diniz, *Adaptive Filtering: Algorithms and Practical Implementation*. Boston, MA, USA: Kluwer, 1997.

[5] R. P. Bitmead and B. D. O. Anderson, "Performance of adaptive estimation algorithms in dependent random environments," *IEEE Trans. Autom. Control*, vol. 25, no. 4, pp. 788–794, Aug. 1980.

[6] R. R. Bitmead, "Convergence properties of LMS adaptive estimators with unbounded dependent inputs," *IEEE Trans. Autom. Control*, vol. 29, no. 5, pp. 477–479, May 1984.

[7] S. C. Douglas, "A family of normalized LMS algorithms," *IEEE Signal Process. Lett.*, vol. 1, no. 3, pp. 49–51, Mar. 1994.

[8] P. S. R. Diniz and L. W. P. Biscainho, "Optimal variable step size for the LMS/Newton algorithm with application to subband adaptive filtering," *IEEE Trans. Signal Process.*, vol. 40, no. 11, pp. 2825–2829, Nov. 1992.

[9] D. Graupe, *Identification of System*. New York, NY, USA: Van Nostrand Reinhold, 1972.

[10] N. Ahmed, D. L. Soldan, D. R. Hummels, and D. D. Parikh, "Sequential regression considerations of adaptive filtering," *Electron. Lett.*, vol. 13, no. 15, pp. 446–448, Jul. 1977.

[11] S. D. Stearns, *Digital Signal Analysis*. New York, NY, USA: Hayden, 1975.

[12] E. R. Love, "Fractional derivatives of imaginary order," *J. London Math. Soc.*, vol. 3, no. 2, pp. 241–259, 1971.

[13] K. B. Oldham and J. Spanier, *The Fractional Calculus: Integrations and Differentiations of Arbitrary Order*. New York, NY, USA: Academic, 1974.

[14] A. C. McBride, *Fractional Calculus*. New York, NY, USA: Halsted, 1986.

[15] K. Nishimoto, *Fractional Calculus: Integrations and Differentiations of Arbitrary Order*. New Haven, CT, USA: New Haven Univ. Press, 1989.

[16] S. Samko, A. A. Kilbas, and O. Marichev, *Fractional Integrals and Derivatives: Theory and Applications*. New York, NY, USA: Gordon and Breach, 1993.

[17] K. S. Miller, "Derivatives of noninteger order," *Math. Mag.*, vol. 68, no. 3, pp. 183–192, Jun. 1995.

[18] S. Samko, A. A. Kilbas, and O. Marichev, *Fractional Integrals and Derivatives: Theory and Applications*. New York, NY, USA: Gordon and Breach, 1987.

[19] N. Engheta, "On fractional calculus and fractional multipoles in electromagnetism," *IEEE Trans. Antennas Propag.*, vol. 44, no. 4, pp. 554–566, Apr. 1996.

[20] N. Engheta, "On the role of fractional calculus in electromagnetic theory," *IEEE Antennas Propag. Mag.*, vol. 39, no. 4, pp. 35–46, Aug. 1997.

[21] M.-P. Chen and H. M. Srivastava, "Fractional calculus operators and their applications involving power functions and summation of series," *Appl. Math. Comput.*, vol. 81, nos. 2–3, pp. 287–304, Feb. 1977.

[22] P. L. Butzer and U. Westphal, "An introduction to fractional calculus," in *Applications of Fractional Calculus in Physics*. Singapore: World Scientific, 2000.

[23] S. Kempfle, I. Schäefer, and H. R. Beyer, "Fractional calculus via functional calculus: Theory and applications," *Nonlinear Dyn.*, vol. 29, nos. 1–4, pp. 99–127, Jul. 2002.

[24] R. L. Magin, "Fractional calculus in bioengineering," *Critical Rev. Biomed. Eng.*, vol. 32, nos. 1–4, pp. 105–193, 2004.

[25] A. A. Kilbas, H. M. Srivastava, and J. J. Trujillo, *Theory and Applications of Fractional Differential Equations*. Amsterdam, The Netherlands: Elsevier, 2006.

[26] J. Sabatier, O. P. Agrawal, and J. A. T. Machado, Eds., *Advances in Fractional Calculus: Theoretical Developments and Applications in Physics and Engineering*. Dordrecht, The Netherlands: Springer-Verlag, 2007.

[27] R. C. Koeller, "Applications of fractional calculus to the theory of viscoelasticity," *J. Appl. Mech.*, vol. 51, no. 2, pp. 299–307, Jun. 1984.

[28] Y. A. Rossikhin and M. V. Shitikova, "Applications of fractional calculus to dynamic problems of linear and nonlinear hereditary mechanics of solids," *Appl. Mech. Rev.*, vol. 50, no. 1, pp. 15–67, Jan. 1997.

[29] S. Manabe, "A suggestion of fractional-order controller for flexible spacecraft attitude control," *Nonlinear Dyn.*, vol. 29, nos. 1–4, pp. 251–268, Jul. 2002.

[30] W. Chen and S. Holm, "Fractional Laplacian time-space models for linear and nonlinear lossy media exhibiting arbitrary frequency power-law dependency," *J. Acoust. Soc. Amer.*, vol. 115, no. 4, pp. 1424–1430, 2004.

[31] E. Perrin, R. Harba, C. Berzin-Joseph, I. Iribarren, and A. Bonami, "Nth-order fractional Brownian motion and fractional Gaussian noises," *IEEE Trans. Signal Process.*, vol. 49, no. 5, pp. 1049–1059, May 2001.

[32] C.-C. Tseng, "Design of fractional order digital FIR differentiators," *IEEE Signal Process. Lett.*, vol. 8, no. 3, pp. 77–79, Mar. 2001.

[33] Y. Chen and B. Vinagre, "A new IIR-type digital fractional order differentiator," *Signal Process.*, vol. 83, no. 11, pp. 2359–2365, Nov. 2003.

[34] Y.-F. Pu, "Research on application of fractional calculus to latest signal analysis and processing," Ph.D. dissertation, School Electron. Inf., Sichuan Univ., Sichuan, China, 2006.

[35] Y.-F. Pu, X. Yuan, K. Liao, Z.-L. Chen, and J.-L. Zhou, "Five numerical algorithms of fractional calculus applied in modern signal analyzing and processing," *J. Sichuan Univ., Eng. Sci. Ed.*, vol. 37, no. 5, pp. 118–124, 2005.

[36] Y.-F. Pu *et al.*, "Structuring analog fractance circuit for 1/2 order fractional calculus," in *Proc. 6th IEEE Conf. ASIC*, Shanghai, China, Oct. 2005, pp. 1136–1139.
[37] Y.-F. Pu, X. Yuan, K. Liao, Z.-L. Chen, and J.-L. Zhou, "Implement any fractional order neural-type pulse oscillator with net-grid type analog fractance circuit," *J. Sichuan Univ., Eng. Sci. Ed.*, vol. 38, no. 1, pp. 128–132, 2006.
[38] S.-C. Liu and S. Chang, "Dimension estimation of discrete-time fractional Brownian motion with applications to image texture classification," *IEEE Trans. Image Process.*, vol. 6, no. 8, pp. 1176–1184, Aug. 1997.
[39] Y.-F. Pu, "Fractional calculus approach to texture of digital image," in *Proc. 8th Int. Conf. Signal Process.*, Nov. 2006, pp. 1002–1006.
[40] Y.-F. Pu, "Fractional differential filter of digital image," ZL Patent 10 021 702, Aug. 30, 2006.
[41] Y.-F. Pu, "High precision fractional calculus filter of digital image," ZL Patent 10 138 742, Apr. 2, 2010.
[42] Y.-F. Pu, W.-X.Wang, J.-L. Zhou, Y.-Y. Wang, and H.-D. Jia, "Fractional differential approach to detecting textural features of digital image and its fractional differential filter implementation," *Sci. China Ser. F, Inf. Sci.*, vol. 51, no. 9, pp. 1319–1339, Sep. 2008.
[43] J. Bai and X.-C. Feng, "Fractional-order anisotropic diffusion for image denoising," *IEEE Trans. Image Process.*, vol. 16, no. 10, pp. 2492–2502, Oct. 2007.
[44] Y.-F. Pu, J.-L. Zhou, and X. Yuan, "Fractional differential mask: A fractional differential-based approach for multiscale texture enhancement," *IEEE Trans. Image Process.*, vol. 19, no. 2, pp. 491–511, Feb. 2010.
[45] Y.-F. Pu and J.-L. Zhou, "A novel approach for multi-scale texture segmentation based on fractional differential," *Int. J. Comput. Math.*, vol. 88, no. 1, pp. 58–78, Jan. 2011.
[46] Y. Pu *et al.*, "Fractional partial differential equation denoising models for texture image," *Sci. China Inf. Sci.*, vol. 57, no. 7, pp. 1–19, Jul. 2014.
[47] Y.-F. Pu, P. Siarry, J.-L. Zhou, and N. Zhang, "A fractional partial differential equation based multiscale denoising model for texture image," *Math. Methods Appl. Sci.*, vol. 37, no. 12, pp. 1784–1806, Aug. 2014.
[48] Y.-F. Pu, J.-L. Zhou, P. Siarry, N. Zhang, and Y.-G. Liu, "Fractional partial differential equation: Fractional total variation and fractional steepest descent approach-based multiscale denoising model for texture image," *Abstract Appl. Anal.*, vol. 2013, pp. 1–19, Aug. 2013, Art. ID 483791.
[49] J. A. Snyman, *Practical Mathematical Optimization: An Introduction to Basic Optimization Theory and Classical and New Gradient-Based Algorithms*. Beijing, China: Springer-Verlag, 2005.
[50] Y.-F. Pu, X. Yuan, K. Liao, J.-L. Zhou, N. Zhang, and Y. Zeng, "A recursive net-grid-type analog fractance circuit for any order fractional calculus," in *Proc. IEEE Conf. Mechatron. Autom.*, Jul./Aug. 2005, pp. 1375–1380.
[51] Y.-F. Pu, "Implement any fractional order multilayer dynamics associative neural network," in *Proc. 6th IEEE Conf. ASIC*, Shanghai, China, Oct. 2005, pp. 638–641.

Yi-Fei Pu received the Ph.D. degree from the College of Electronics and Information Engineering, Sichuan University, Chengdu, China, in 2006.

He is currently a Professor and Doctoral Supervisor with the School of Computer Science and Technology, Sichuan University, and was elected into the Thousand Talents Program of Sichuan Province. He focuses on the application of fractional calculus and fractional partial differential equation to signal analysis and processing. He has authored about 20 papers indexed by SCI in journals such as the IEEE TRANSACTIONS ON IMAGE PROCESSING, *Mathematic Methods in Applied Sciences*, and *Science in China Series F: Information Sciences*. He held several research projects, such as the National Nature Science Foundation of China and the Returned Overseas Chinese Scholars Project of Education Ministry of China, and holds six China Inventive Patents, as the first or a single inventor.

Ji-Liu Zhou (SM'10) received the Ph.D. degree from Sichuan University, Chengdu, China, in 1999.

He is currently a Professor and Doctoral Supervisor with the School of Computer Science and Technology, Sichuan University, Chengdu. He is also the Academic and Technical Leader and the outstanding expert of Sichuan Province, and has held 17 state or provincial scientific projects, including key projects supported by the National Science Foundation. His current research interests include image processing, artificial intelligence, fractional differential application on the latest signal, and image processing. He has authored over 100 papers, of which over 80 papers are indexed by SCI, EI or ISTP.

Yi Zhang (SM'01) received the Ph.D. degree from the Institute of Mathematics, Chinese Academy of Sciences, Beijing, China, in 1994.

He is currently a Professor, a Doctoral Supervisor, and the Dean of the School of Computer Science and Technology with Sichuan University, Chengdu, China. He is supported by the Program for New Century Excellent Talents in University, an outstanding expert of Sichuan Province, and received the National Prize for progress in science and technology issued by the Ministry of Education of China in 2012. He has held some projects, such as the National Key Basic Research and Development Plan (973 Plan), the National High Technology Research and Development Program 863, and the National Nature Science Foundation of China. He has authored over 30 papers in the IEEE TRANSACTIONS series, and 128 papers are indexed by SCI.

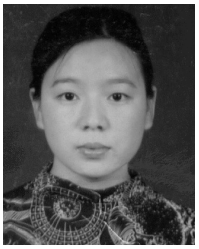

Ni Zhang received the Ph.D. degree from the South Western University of Finance and Economics, Chengdu, China, in 2012.

She is currently a Librarian with the Library of Sichuan University, Chengdu. She is interested in application of fractional calculus to signal analysis and processing and took part in some of related projects. She has authored over ten papers, three indexed by SCI, four indexed by EI, and four indexed by CSSCI. Her current research interests include the interdisciplinary field of artificial intelligence and law, in particular, semantic information retrieval of legal knowledge.

Guo Huang received the Ph.D. degree from the School of Computer Science and Technology, Sichuan University, Chengdu, China, in 2011.

He is currently an Associate Professor with the College of Computer Science and Technology, Leshan Normal University, Leshan, China. His current research interests include applying fractional calculus and fractional partial differential equations on image enhancement, denoising, and segmentation.

Patrick Siarry (SM'95) is currently a Professor and a Doctoral Supervisor of Automatics and Informatics with the University of Paris-Est Créteil, Créteil, France. He is the Head of one team of the Laboratoire Images, Signaux et Systèmes Intelligents, University of Paris-Est Créteil. He supervises a Research Working Group, in the frame of Centre National de la Recherche Scientifique, META, since 2004. META is interested in theoretical and practical advances in metaheuristics for hard optimization. His current research interests include improvement of existing metaheuristics for hard optimization, adaptation of discrete metaheuristics to continuous optimization, hybridization of metaheuristics with classical optimization techniques, dynamic optimization, and particle swarm optimization.